Additive Manufacturing 27 (2019) 451–460

Contents lists available at ScienceDirect

Additive Manufacturing

journal homepage: www.elsevier.com/locate/addma

Parallel electrostatic grippers for layered assembly

Joni Mici*, Jang Won Ko, Jared West, Jeffrey Jaquith, Hod Lipson

Columbia University, Department of Mechanical Engineering, 500 W 120th Street, Mudd #220, New York, NY, USA

ARTICLE INFO

Keywords:
Additive manufacturing
Electrostatic gripper
Electroadhesion
Layered assembly
Voxel printing
Multi-material

ABSTRACT

Layered Assembly is a voxel-based additive manufacturing method in which premanufactured voxels serve as the feedstock for producing multi-material parts. The parallel placement of voxels necessary for Layered Assembly is carried out by electroadhesion—a type of astrictive prehension, which is an elegant, scalable, low-power, solid-state, and epoxy-free grasping method with numerous applications. In the present work, 2 × 2 arrays of electroadhesive grippers were designed in both comb- and spiral-shaped electrode geometries. Electrodes were nominally designed for grasping voxels of 3 × 3 mm cross-section. Electrostatic field simulations were performed in COMSOL Multiphysics for both single electrodes, and 2 × 2 electrode arrays. The selective gripping capability of the electrode arrays was tested at voltages in the 75–800 V range and applied to both polymer and metallic voxels. A comparison of electrode performance in terms of geometry revealed that comb-shaped electrodes were superior, due to ≈100% reliability when operating in the 600–800 V range.

1. Introduction

1.1. Multi-material additive manufacturing

Most of the additive manufacturing (AM) processes currently in use are unsuitable for fabrication of dissimilar materials in the same build process. While progress has been made in multi-polymer AM [1,2], and multi-metal AM [3,4], material chemistry fundamentally prevents established AM processes, nominally PolyJet, Powder Bed Fusion, and Directed Energy Deposition, from co-fabricating parts comprised of metals and polymers in the same build tray. To highlight these material science limitations, consider that some of the most advanced 3D printers can manufacture FAA-qualified fuel nozzles [5], yet cannot fabricate a handheld TV remote.

One way to broadly address this multi-material challenge is to fine tune the properties of dissimilar materials to allow their co-fabrication using established AM processes, such as those based on Material Extrusion [6]. This approach was examined by Malone et al. [7], who focused on its utility in the freeform fabrication of batteries and conductive wiring in assemblies using a single FDM-like process. More recently, Muth et al. [8] demonstrated the capability of printing strain sensors in soft elastomers using an FDM-like process.

While these and other researchers have achieved some degree of success, the methods they adopted suffer from two fundamental limitations. First, sought-after material properties, such as high conductivity and stiffness, are often compromised to achieve in-printer compatibility. Second, as the resolution of most multi-material AM processes is still relatively low, only relatively crude structures, such as circuit interconnects, can be manufactured. Owing to these issues, printing functional electro-mechanical systems remains a challenge.

Looking forward, successful multi-material printing will pave the way for the production of smart structures containing sensors, actuators, and microprocessors, as well as power and logic components. Thus, the aforementioned drawbacks must be overcome by designing a new AM process which can be employed in the fabrication of even the most complex components requiring optimized nanofabrication processes that have been perfected for decades. In this work, Layered Assembly (LA) is introduced, as a potential candidate to broadly address the multi-material limitations of current additive manufacturing approaches.

1.2. Layered assembly

Layered Assembly (LA) is an additive manufacturing method which systematically builds multi-material parts through layer-by-layer deposition of 3D building blocks knowns as “voxels”. By using voxels in place of the raw material, Layered Assembly fundamentally differs from established AM processes [6] in how the raw material is shaped, manufactured, assembled, and ultimately thought about in design paradigms. The discrete and digital nature of the voxels used in Layered

* Corresponding author.
E-mail addresses: jm4314@columbia.edu (J. Mici), jk3960@columbia.edu (J.W. Ko), jdw2194@columbia.edu (J. West), jfj2122@columbia.edu (J. Jaquith), hl2891@columbia.edu (H. Lipson).

https://doi.org/10.1016/j.addma.2019.03.032
Received 9 January 2019; Received in revised form 19 March 2019; Accepted 26 March 2019
Available online 27 March 2019

Assembly, starkly contrast the continuous filament, resin, or powder melt pools used in established AM processes. Lastly, and most importantly, LA differs from existing multi-material AM methods because it enables the co-fabrication of parts comprised of both metals and polymers in the same build tray.

Owing to their small scale, voxels can be assembled into a wide range of geometries to produce recyclable and modular electromechanical components, which in turn comprise a complex, multi-material product. In LA, voxels serve as feedstock, replacing the traditional raw materials in the manufacturing process. As voxels are independent of the final product characteristics, they can be equipped with microprocessors or batteries, extending their functionality beyond what is associated with their intrinsic material properties [9]. Moreover, voxels can be reused, making LA a more cost-effective process and paving the way toward sustainable manufacturing [10,11].

Each type of voxel used in the LA process can be mass-produced separately by traditional optimized methods. When fabricating multi-material products, voxels of required design and functionality are assembled akin to building blocks using a pick-and-place style robot to produce multi-material systems of virtually unbounded complexity. Such voxel-based structures have been termed “digital materials” by industry practitioners [12] and academic researchers [11,13]. Table 1 shows the relationship between different voxel types and the design space afforded by their use. Clearly, as the number of distinct types of voxels expands, the design scope grows exponentially. As demonstrated in nature, even a small range of distinct building blocks can give rise to a virtually unlimited number of unique designs, as only 22 amino acids were sufficient for the emergence of the immense diversity of biological life on Earth [9]. Once the goal of harmoniously assembling multi-material structures has been attained, printing fully functioning systems, such as robots, will be possible, thus bringing AM to its logical conclusion [10]. Two examples of fully functioning electromechanical systems are shown in Fig. 1, where a relatively small number of voxel types is employed to produce vastly different objects, in this case a smartphone, and an insect-like walking robot—both comprised of over one million voxels. Thus, it is easy to envisage the vast potential of this approach as the range of voxel types expands and the technology advances further.

Another benefit of LA is the possibility of manufacturing objects using self-alignment, as this enables constructing objects that are more precise than the machine that built them. The important consequence of this paradigm shift is that the burden of precision is no longer on the machine, but rather the feedstock, which is easier to control. The self-alignment concept is utilized exceptionally well in the LEGO™ brick design, which ensures that all individual components are compatible and can be used to build an infinitely large number of complex structures of much higher precision than that characterizing the hand that built them. Owens et al. [14] achieved ~1 μm stacking precision with their LEGO™-based microfluidics system. In their approach, microfluidic channels are micro-milled into LEGO™-like bricks before being snapped together to build intricate microfluidic architectures. To extend the functionality range, LEGO™ bricks can be equipped with microprocessors, to combine the benefits of self-alignment with those of modular electromechanical architecture. Such modular

Table 1
Different voxel types and the design spaces they enable [9].

Voxel Type	Design Space
Structural + Support voxels	Arbitrary geometries
+ Soft voxels	Graded materials
+ Conductor voxels	3D Interconnect
+ Resistors, transistors, capacitors	Analog 3D circuits
+ Batteries and PV voxels	Power handling
+ CPU / FPGA voxels	Embedded intelligence
+ Sensor, actuator voxels	Fully operational robots

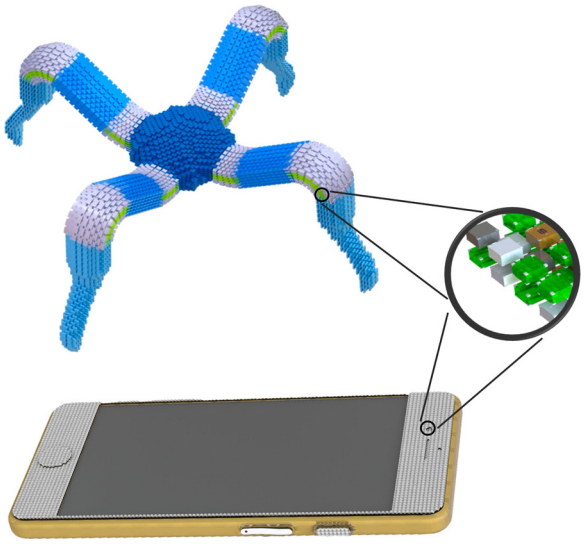

Fig. 1. Layered assembly concept: Illustration of (a) a crawling robot and (b) a smartphone, both comprising of millions of building blocks from a small repertoire of functional types, namely structural, electrical, light emitting, and actuating.

electromechanical architectures were proposed by Gershenfeld [15], who is of view that the benefits of digital materials are largely unexplored and that LEGO™-style materials and architectures have immense manufacturing potential.

1.3. Parallelization: bringing Moore’s law to digital manufacturing

In LA, resolution can be improved by reducing voxel size and increasing voxel count, which can only be achieved by parallel voxel placement to maintain speed when the process is scaled-up. For example, a million-voxel-class assembly would require twelve days to assemble on leading pick-and-place systems, such as the M2-*i*A robot made by FANUC America Incorporated [16]. Unless process scalability is vastly improved, a billion-voxel assembly would take nearly a year, as the total assembly time using a serial pick-and-place process increases linearly with voxel count. This example aptly illustrates the necessity of a parallel process that can considerably shorten the manufacturing time.

The proposed LA process addresses this issue effectively, as the time required for assembly increases as the cube root of the number of voxels required. Moreover, optimizing the use of parallel arrays allows LA to scale with the number of layers, rather than the number of voxels, which is highly beneficial, given that the difference between linear and cube root scalability grows rapidly with the increase in the number of voxels required for assembly.

In order to realize a highly parallel assembly process, the optimal LA gripper arrays must be mechanically robust, scalable, and compatible in a wide variety of environments, including outer space, while requiring low power. In pursuit of this goal, as a part of the work presented here, the potential for parallelizing the pick-and-place assembly process through the use of parallel gripper arrays was investigated.

1.4. Electroadhesion

Robotic grippers are typically classified as astrictive, ingressive, impactive, and contiguitive. Astrictive processes, for example, require fields—which could be a pressure field (e.g., partial vacuum), electrostatic, or electromagnetic—to produce binding forces. Contiguitive grippers, on the other hand, achieve prehension via thermal and chemical effects and thus require direct contact between the gripper and object surfaces. Impactive grippers achieve prehension by applying

mechanical forces to the surface of the intended object. Finally, ingressive grippers permeate the surface of the target object to achieve prehension [17]. At present, impactive and astrictive grippers are the most commonly used in the automation industry [18].

Since gripping strength of astrictive methods is proportional to the surface area, they are better suited for gripping smaller parts, which inherently have higher surface area-to-mass ratios. In the present study, electroadhesion was adopted, since it can be implemented with solid-state circuits. In addition, it scales well to parallel arrays, and is compatible with both conducting and non-conducting materials. However, it is worth noting that electro-osmosis methods have also been investigated for parallel pick-and-place application [19,20]. Nonetheless, as electroadhesion requires relatively little hardware compared to other astrictive prehension methods, like vacuum and electro-osmosis, it was deemed the most optimal choice for the present investigation. Additionally, electroadhesion exhibits ultra-low power consumption and is compatible with the conditions in outer space [21–23]. Electroadhesion is particularly well suited for use in vacuum, as electrodes are less susceptible to arcing, thus ensuring higher gripping strength. Batra et al. [24] explored the possibility of in situ voxel construction beyond Earth's atmosphere, indicating that electroadhesive grippers can have a wide range of applications in vacuum.

Electroadhesion is the electrostatic effect of astriction that occurs between two surfaces subjected to an electric field. In the implementation described in this work, electroadhesion occurs between an electroadhesive pad generating high electric field gradient and the separated charges in the target object—in this case a voxel. When plates with high positive and negative electric potential are in close proximity, a steep electric field gradient is generated. This field gradient causes any free electric charges in the vicinity to separate into positive and negative clusters. This includes any object within that field, and thus the voxel and the electrodes themselves. Upon separation, negative charges in voxels will be attracted by a positively charged electrode, and vice versa, creating an attraction force.

Electroadhesion is a complex phenomenon. To date, 33 independent factors influencing process success have been identified ranging from intrinsic material properties (such as dielectric permittivity) to environmental factors (such as humidity and barometric pressure) [25]. Both conducting and non-conducting materials can be subject to electroadhesion, albeit based on different physics phenomena. In conductive materials, electroadhesive forces are generated mainly by electrostatic induction, while polarization is the source of electroadhesive forces in non-conductors [22].

In their study, Ruffato et al. [26] performed FEA-based 2D optimization of the electrode geometries of centimeter-scale electroadhesive grippers intended for bio-inspired wall climbing robots. They conclude that highly interdigitated spiral electrode geometries are optimal for cm-scale robotic grippers. While the study is subject to different manufacturing constraints than this work, it served as a starting point for some of the electrode geometries in this study, albeit for mm scale rather than cm scale. The grasping of smaller objects is studied by Monkman et al. [27] showing promising results on the utility of electroadhesive microgrippers in grasping arbitrarily shaped sub-millimeter sized objects. Despite the advances made by these and other authors, parallel electroadhesive gripper arrays have not been explored in extant studies, leading to a gap in pertinent models, control strategies, and design paradigms. This gap in the extant knowledge has motivated the present work, the aim of which was to demonstrate the design and implementation of a gripping array.

Fig. 2 shows an illustration of a 32 × 32 electrostatic gripping array selectively holding as many as 1024 voxels of an arbitrary configuration. Extrapolating from this example, it is evident that a set of nine such arrays in a 3 × 3 configuration could assemble up to 9216 voxels per layer. Assuming that one layer can be assembled per minute, 1 million voxels would be correctly placed within two hours. In this paper, we report on the implementation of a 2 × 2 array, as the first step towards 1024-voxel array fabrication. We commence the discussion by describing the construction of the electrostatic electrodes, followed by their scalability and reliability analyses. The experimental work reported in this paper aimed to demonstrate the manufacturing methods employed, as well as validate the performance of the proposed design in terms of polymer and metallic voxel gripping success.

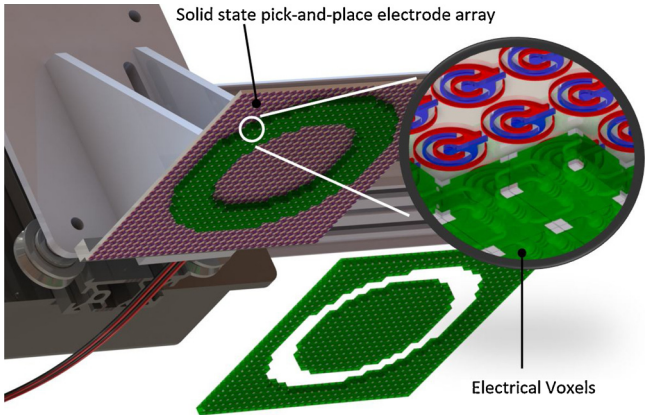

Fig. 2. Rendering of a Layered Assembly machine equipped with a 32 × 32 electrode array selectively gripping a circular shape out of an array of voxels.

2. Materials and methods

2.1. Single electrode design

A cross-section of a basic electroadhesive gripper is shown in Fig. 3. The highest electric field density, which corresponds to the maximum electroadhesive strength, is attained in the gap between the positive and negative plates. The design intent is to maximize electric field density throughout the gripper surface, and therefore maximize the length of this gap, denoted as *interdigitation length*. This design objective necessitates highly interdigitated electrode geometries, as shown in Fig. 4. Interdigitated electrode geometries have been explored in extant optimization studies, as a part of which researchers adopted varied manufacturing methods, at different scales, aimed at diverse applications [28,29].

Electroadhesive grippers were designed for maximum interdigitation length, for traces bounded in a 3 × 3 mm design space. The limiting factor was the minimum machinable channel width, estimated at .010", corresponding to the smallest commercially available endmill. Renderings of the two resulting electrode array designs are depicted in Fig. 5.

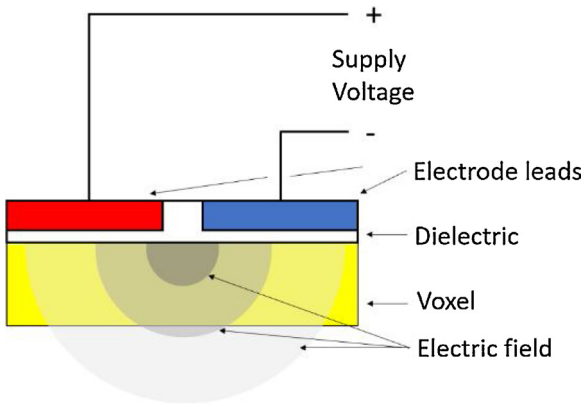

Fig. 3. Basic anatomy of an electroadhesive gripper (for a dielectric voxel, the dielectric layer may be removed).

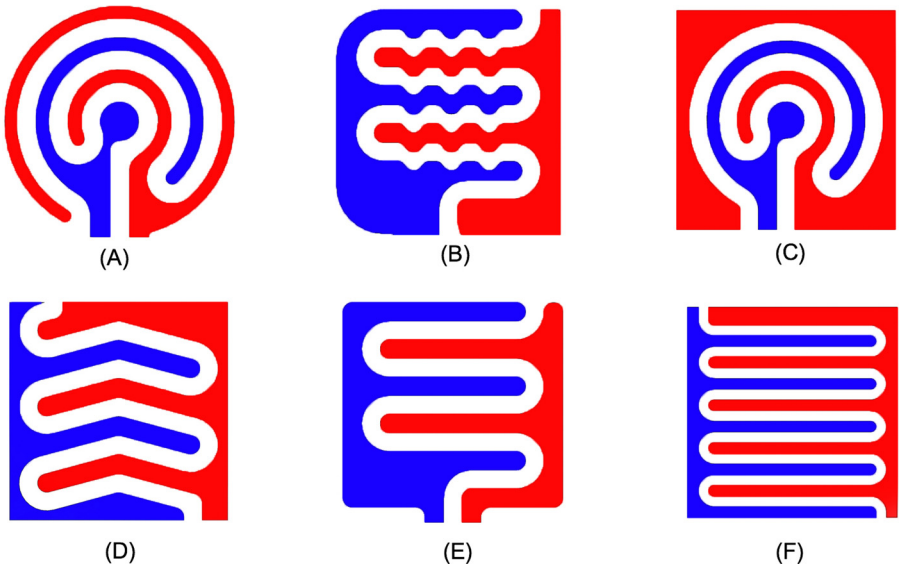

Fig. 4. (A) Interdigitated spiral design with .010" spacing. (B) A squiggly comb with .010" trace spacing. (C) Interdigitated spiral design with .010" spacing, and filled in background. (D) A Chevron-shaped comb design with .010" spacing. (E) An interdigitated spiral design with .010" spacing. (F) Comb electrode design with .010" trace spacing, and (F) a comb electrode design with .006" spacing.

2.2. Electrode array design

The electrode from Fig. 4A and E were configured in the alternating 2 × 2 pattern shown in Fig. 5, thus differing from that depicted in Fig. 2, which is closely packed with electrodes. These electrode geometries were chosen for experimental validation as they are fundamentally different geometries. The sparse 2 × 2 pattern was chosen in this particular case (1) to facilitate trace routing, (2) ensure superior material handling, and (3) allow for more selective pick-and-place operations. Such checkerboard-like patterns are desirable, as most electromechanical systems will inherently require interspersed voxels to aid in cooling, as seen in the insect-like robot in Fig. 1. Interspersed electrode placement is also beneficial for desensitizing the Layered Assembly process to voxel imperfections. To achieve 100% infill, checkerboard style systems such as the one shown here will need to perform three pick-and-place operations per layer.

2.3. Analysis

Finite element analysis was performed in a COMSOL Multiphysics simulation environment for six unique single electrodes (Fig. 4) and the two 2 × 2 electrode arrays (Fig. 5). Six single electrode geometries were considered as is shown in Fig. 4. For each simulation the average electric field was calculated at the face of the electrode traces, representative of the location where it would contact an intended voxel. Analysis results of single electrodes informed the design, selection and manufacturing of the 2 × 2 electrode array.

2.3.1. Single electrode analysis

The best performing electrode was the comb shaped electrode with .006" trace spacing, corresponding to an average electric field of 1.66 MV / m as seen in Fig. 6F. We attribute this optimal performance to high interdigitation length, and closely spaced traces. While the comb shaped electrode in Figs. 4F, 6 F is the optimal electrode in simulation, it is not possible manufacture with a CNC desktop mill and was not manufactured in this work.

2.3.2. Analysis of electrode array

While the single electrode simulations informed electrode geometry selection for optimal electric field strength, the simulation for the 2 × 2 electrode arrays is meant to show the selective capabilities of the array. Specifically, the analysis sought to answer how much lower the electric field was outside of the intended gripping area. To quantify the electric field decay outside of the active electrode area, we averaged the electric field at a central cross section of the electrode array. The plots of these cross sections are shown in Fig. 7B and D, respectively. The electric field of inactive areas adjacent to the square comb electrode traces is 86% lower, whereas for the spiral electrode it is 68% lower. Moreover,

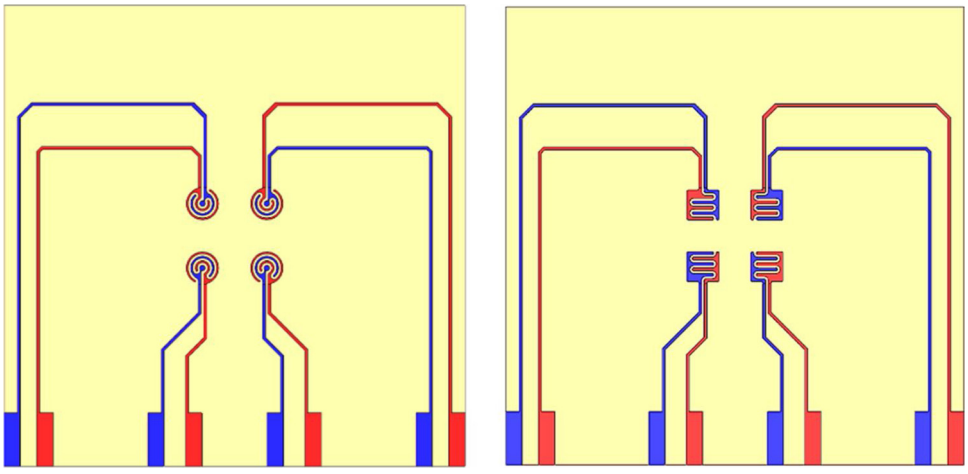

Fig. 5. CAD rendering of (A) a spiral electrode array, and (B) a comb electrode array. Both electrodes have 0.010" spacing between the leads.

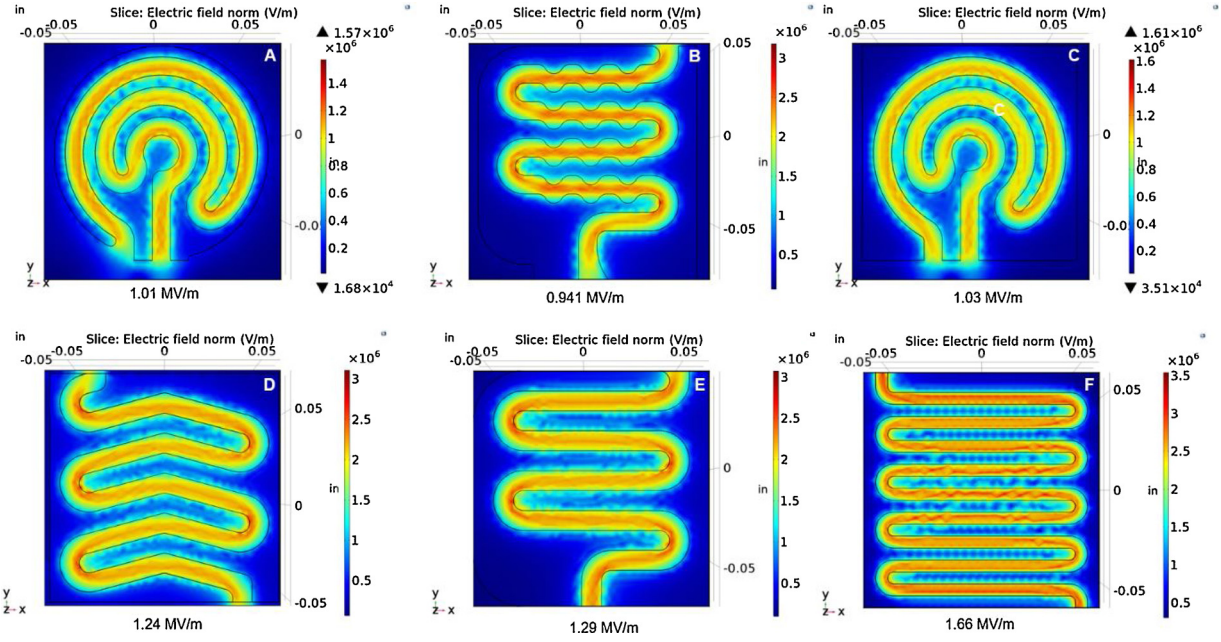

Fig. 6. (A) - (F) COMSOL Simulations of electrostatic fields corresponding to Fig. 4(A)–(F).

comparing Fig. 7B–D, we see the electric field of the comb electrode is much more constant over the active electrode area. This may explain why the comb shaped electrodes excel at grasping voxels at large misalignments.

2.4. Electrode manufacturing

Electrodes utilized in the present study were manufactured on a desktop CNC mill (OtherMill Pro) using endmill diameters ranging from .010" to 0.125". To optimize the surface finish of electrode traces, finishing passes were employed. Additionally, an on-board vacuum

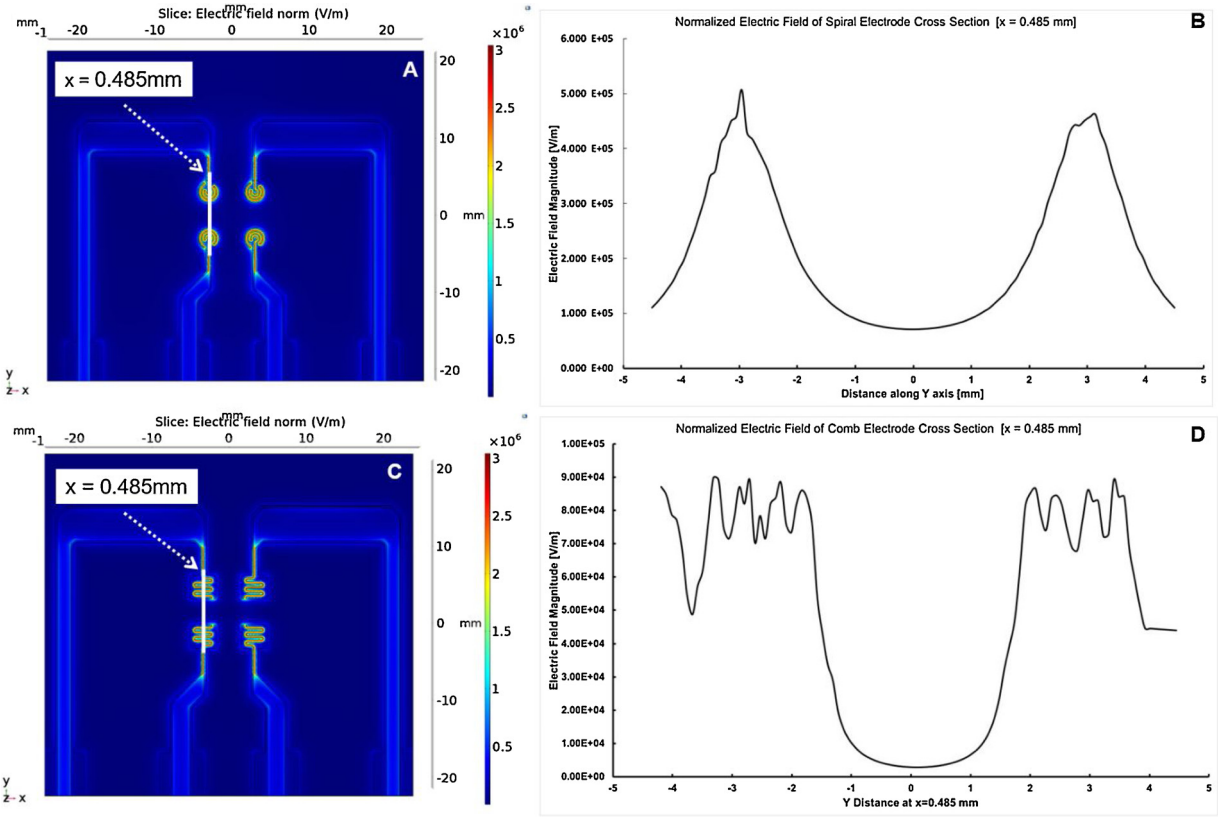

Fig. 7. COMSOL Simulation results of electrode arrays. (A) Normalized electric field plot of 2 × 2 spiral electrode array. (B) Plot of normalized electric field for spiral electrodes at x = 0.485 mm cross section. (C) Normalized electric field plot of 2 × 2 comb electrode array. (D) Plot of normalized electric field for comb electrodes at x = 0.485 mm cross section.

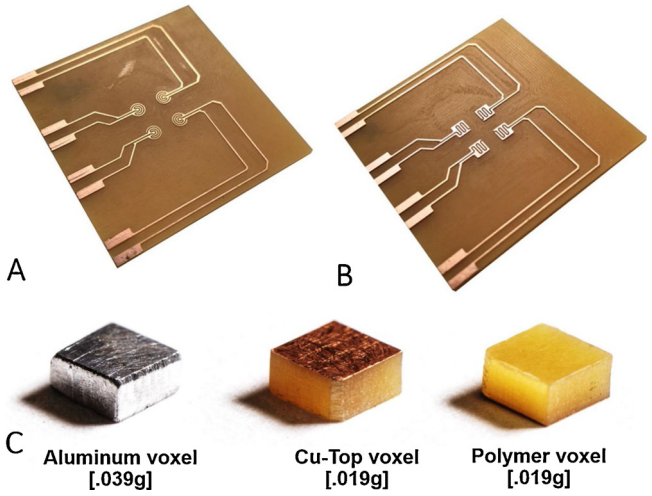

Fig. 8. An example of a manufactured (A) 2 × 2 spiral electrode array, and (B) 2 × 2 a comb electrode array. (C) Metallic, metal-topped, and polymeric voxels.

fitting was used to assist with in situ chip removal. Electrodes were fabricated from single-sided FR1 boards. Following milling, electrodes were tested for continuity between traces. The as-manufactured electrodes are depicted in Fig. 8A and B, while the 3 × 3 mm voxels used in the study are shown in Fig. 8C.

2.5. Testing

2.5.1. Maximum allowable voltage

Electrode arrays were tested to failure by gradually increasing the applied voltage. Failure was defined as the voltage at which arcing occurs and the electrode loses its gripping capability. While electrodes

Table 2
Reliability testing procedure adopted for 2 × 2 electrostatic grippers.

1	Randomly position four voxels on the alignment jig
2	Align the jig with the electrode
3	Apply high voltage [75–800 V]
4	Move gantry down to apply 3 N of normal force to voxels at an approach speed of 100 mm / min
5	Dwell for 1.0 s
6	Move gantry up at 200 mm / min to the final height of 8 mm
7	Count the successfully grasped voxels
8	Turn off the voltage supply

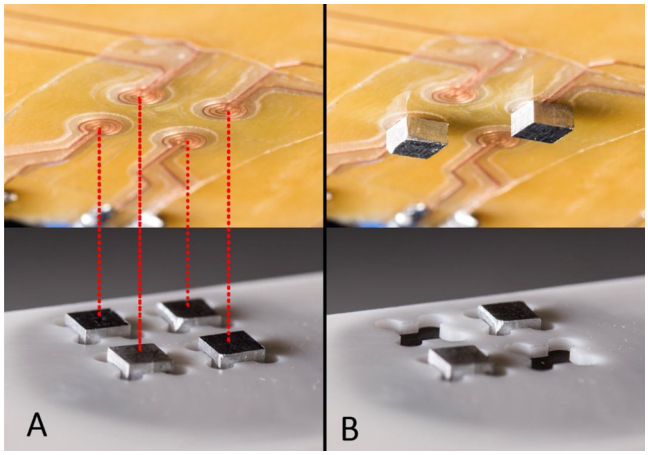

Fig. 10. Voxels in the test rig. (A) Four voxels placed in the alignment jig, awaiting pickup. (B) Following contact, the electrode array selectively picks up two of the four voxels on the jig.

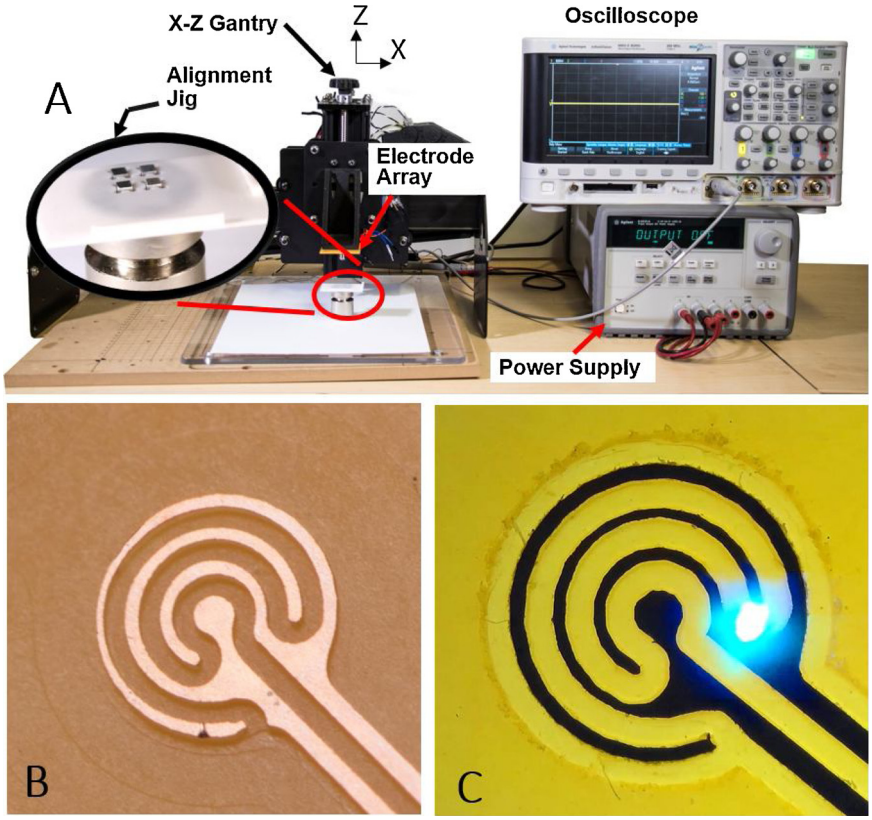

Fig. 9. (A) Testing setup, zooming in on the alignment jig. (B) Close-up view of as-manufactured spiral electrode. (C) Spiral electrode shorting at a point of high curvature.

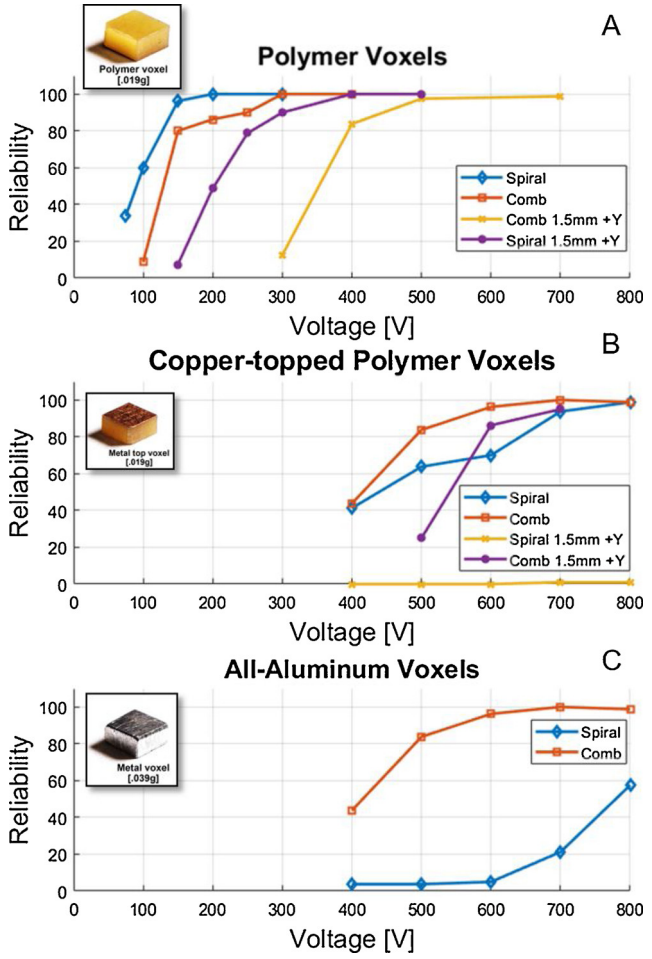

Fig. 11. (A) Gripping reliability of a bare electrode when applied to polymeric voxels. (B) Gripping reliability of a Teflon-coated electrode array when used to collect polymeric voxels with copper tops. (C) Gripping reliability of Teflon-coated electrode array when attempting to collect Al voxels.

with poorer surface finish were more susceptible to arcing at lower voltages, arcing occurred at 900–1200 V irrespective of the electrode type. As shown in Fig. 9C, arcing occurred in areas of high curvature change, such as the electrode tips. Knowledge of this failure mode can aid in future electrode design and geometry optimization.

2.5.2. Testing setup

As shown in Fig. 9A, electrode arrays were connected to a high voltage transformer (Sunkee #CECOMINOD00 5509) powered by an Agilent E3631 A Triple Output Power Supply. High voltage was measured by a Keysight 10076C High Voltage Probe. The electrode board was then secured to the gantry of an X-carve CNC system capable of 75 μm axial precision [30]. The electrode board was attached to the gantry using compressible 2 mm thick VHB 3 M tape. By allowing the electrode array some degree of movement, the compressible tape desensitized the system to ± 2° tip / tilt misalignment errors, while also ensuring that each voxel achieves flush contact with its respective electrode leads.

To ensure adequate alignment in the *xy* plane, an alignment jig, also depicted in Fig. 9A, was machined. The jig is equipped with two reference surfaces to help locate the voxels with respect to the electrodes. To achieve this objective, the reference surfaces were manually placed at tangent to the electrode board prior to each trial. As shown in the setup rendering, the white bracket of the jig is positioned on two layers of 1 mm thick neoprene foam to allow independent vertical movement of voxels. This movement maximizes surface-to-surface contact between voxels and electrodes and further desensitizes the system to tolerance stack-ups between the electrode array and voxels. The voxels used in electrode array trials conducted as a part of this investigation are shown in Fig. 8C, which depicts (1) a polymeric voxel, (2) polymeric voxel with a metal top, and (3) an aluminum voxel.

2.5.3. Testing procedure

Electrode arrays were covered with Teflon tape to enable the adhesion of conducting voxels. Each trial consisted of 20 attempts of simultaneously picking up four voxels from the jig. A video recording of the voxel pick up is included in the references [31], while selected video frames are included in Appendix A. The steps involved in the testing procedure are presented in Table 2.

At the beginning and end of each trial, dry runs were performed to check for false positive pickup, which occurred when using masking tape as the dielectric medium. The issue of false positives was mitigated by using Teflon tape with a silicone adhesive. After each pickup attempt, the collected voxels were taken out of the jig and randomly replaced to simulate the machine encountering a new layer of voxels in the Layered Assembly process. Four voxels on the alignment jig are shown in Fig. 10A, while Fig. 10B shows a pickup attempt in which only two voxels were collected.

3. Results

3.1. Gripping reliability tests

Gripping reliability was the main objective of the present study, as it must be guaranteed for the LA to advance forward. In the context of the current investigation, reliability was defined as the ratio of collected voxels to the number of attempted pickups. Specifically, a pickup was deemed successful when a voxel is gripped for 1 s or longer at a height of 8 mm above the voxel jig (further details are given in the supplementary materials).

3.1.1. Centered voxels

The gripping reliability of voxels that were centered to their respective electrodes is shown in Fig. 9A. These trials represent nominal testing conditions, in which the electrodes are aligned to +/− 0.1 mm of their intended voxel. As can be seen from the graph, spiral electrodes outperformed comb electrodes at lower voltages, and asymptotically approached 100% gripping reliability at 300 V. However, when electrodes were covered with a dielectric (Teflon tape), comb electrode arrays outperformed the spiral electrode arrays. The dielectric-covered array is a more realistic configuration, as electrodes in the Layered Assembly process must be able to handle both conductive and non-conductive materials.

3.1.2. Misaligned voxels

We also tested gripping reliability at 50% voxel-electrode misalignment in the *y*-axis direction and the results are reported in Fig. 11A and B. Such large misalignment was intentionally chosen to explore the possibility of the electrode arrays gripping voxels or parts that are of a relatively bigger size, or uneven integer multiples of the checkerboard-style spacing. These results will also benefit further research into designs required for picking up hierarchal voxel geometries, as well as parts of arbitrary shapes. As can be seen from the graphs, performance of comb electrodes was superior to that of spiral electrodes under all testing conditions.

3.2. Optimal electrodes and voltage ranges

The results obtained in the present study suggest that comb electrodes with a Teflon tape dielectric are the optimal geometry for multi-material grasping. Furthermore, these results indicate that the necessary voltage for effective and reliable multi-material gripping is in the

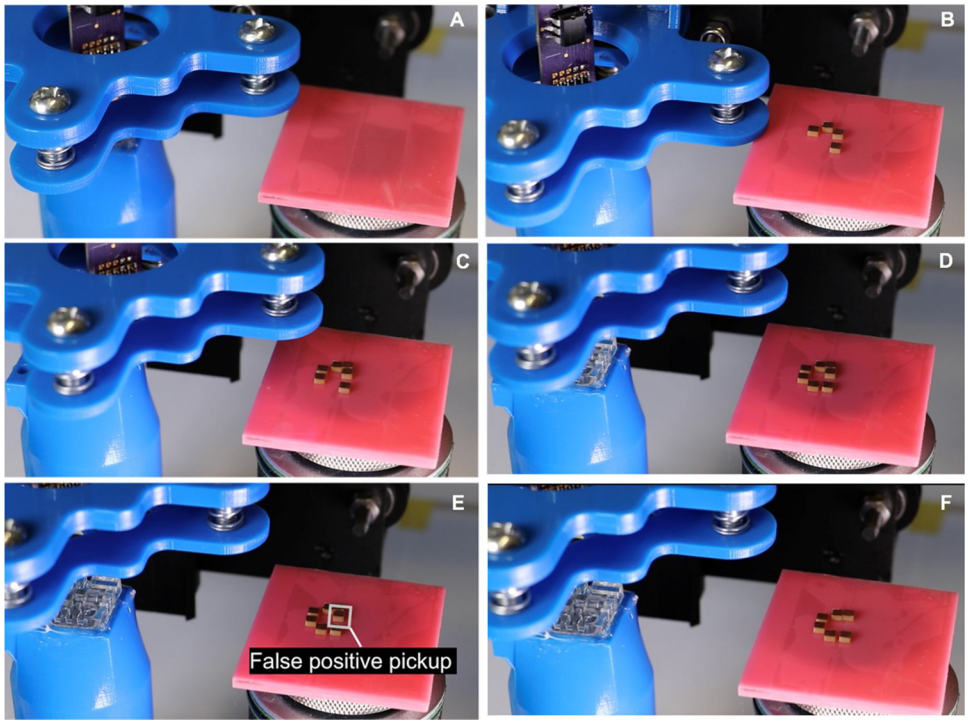

Fig. 12. (A) The beginning of the processes: an empty tray in pink, and a blue deposition head. (B) Completed placement of first batch of voxels. (C) Completed placement of second batch of voxels. (D) Completed placement of third batch of voxels. (E) Extra voxel is noticed and removed. (F) Final discretized "C". (For interpretation of the references to colour in this figure legend, the reader is referred to the web version of this article).

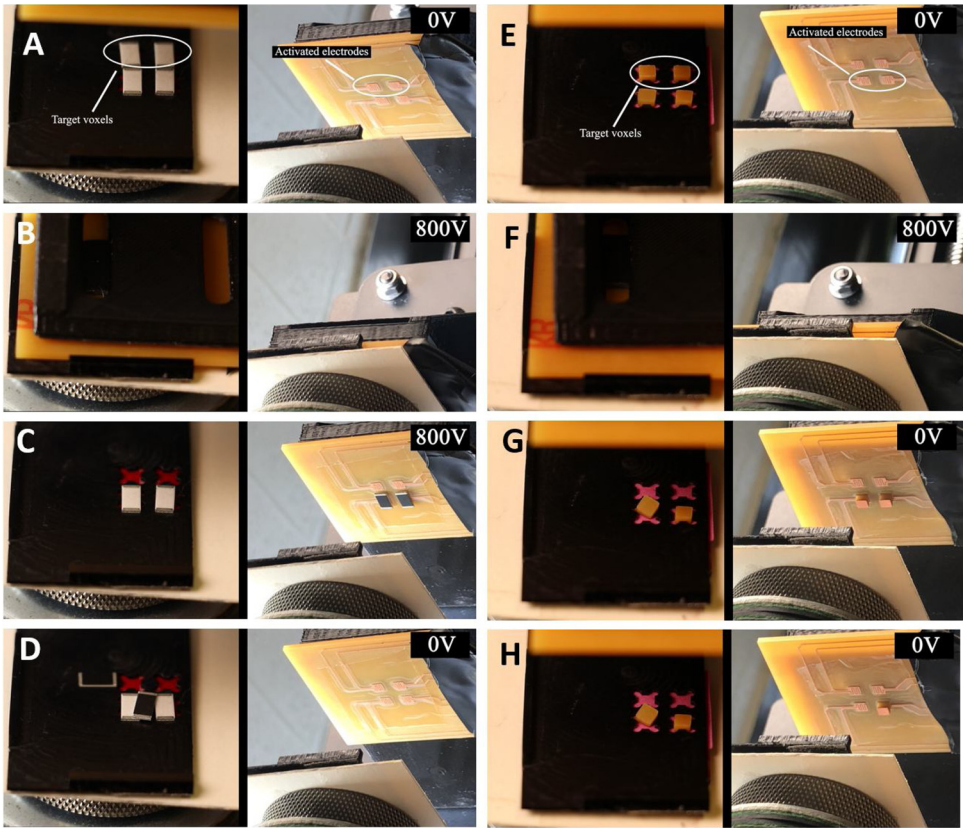

Fig. 13. (A) The beginning of the grasping process for SMT resistors. (B) Electrode array is lowered to contact resistors surfaces. (C) Electrode array selectively grips intended resistors. (D) Voltage is turned off and resistors drop. (E) The beginning of the grasping process for polymer voxels. (F) Electrode array is lowered to contact voxel surfaces. (G) Electrode array selectively grips intended voxels. (H) Voltage is turned off and polymer voxels drop.

600–800 V range. We therefore conclude that comb geometry is the optimal geometry for multi-material electroadhesive grippers for parallel pick-and-place maneuvers commonly employed in LA.

3.3. Building a part

To demonstrate the additive manufacturing capabilities of Layered Assembly, a discretized letter "C" was manufactured out of copper-topped voxels as seen in Fig. 12F. The "C" was comprised of three separate pick and place operations shown in Fig. 12B–D. A false positive pick-and-place was recorded (Fig. 12E), and manually removed. After all voxels were placed on the build tray, voxels were sprayed with an acrylic coating to bond them together. Layered Assembly is not limited to acrylic coating, as the coating could easily be changed to match the

needed form and function. The entire build process is shown in Movie S2.

3.4. Grasping circuit components

In addition to the discretized letter “C”, this work explored the capability of electrode arrays to grasp commercially available components such as the surface-mounted resistors shown in Fig. 13. Towards this, selective pickup was effectively demonstrated for these resistors as seen in Movie S3. This capability has important implications for the employment of Layered Assembly both as a novel additive manufacturing method and a parallel pick-and -place technology for placing electronic components on circuit boards.

4. Discussion

4.1. Optimal geometry

Based on the findings obtained in the present study, comb electrodes appear to be the more effective geometry relative to the spiral design when considered for the checkerboard-style packing required for parallel voxel assemblies. They are more effective at gripping with dielectric insulators and more robust against large electrode–voxel misalignments. Large misalignment performance is largely dependent on the routing of traces leading up to the electrodes since when misaligned voxels contact traces, the traces effectively act as electrodes. The testing conducted in the present study shows that the comb (and potentially spiral) electrode arrays could also be well adapted to picking up arbitrary cross-sections, increasing their usefulness in other pick-and-place applications. Specific to LA, comb electrodes can be positioned more efficiently in a checkerboard array and are easier to manufacture relative to the spiral design. Although comb electrodes have shorter interdigitation lengths than the spiral electrodes, they utilize more of the bounding box area (Fig. 4), which we postulate to be the primary determinant of their superior performance. These assertions and other results reported in this paper can be further confirmed with finite element simulations of electrostatic fields, as one of the fruitful avenues for future LA research.

4.2. Future work

Gripping reliability demonstrated in this work could be further improved by enhancing the electrode flatness, and thereby increasing the surface-to-surface contact between electrode and voxel. This can be achieved by adding fillers between electrode traces, allowing for more uniform contact between the dielectric strip and the electrode surface. Going forward, we plan to investigate the effects of dwell time, compression, and alternating voltage, as these parameters could potentially enhance gripping reliability. In addition, they may facilitate gripping at lower voltages, which would improve safety and cost effectiveness, as well as reduce transistor size and complexity. Finally, gripper reliability can also be improved by the implementation of both manual and automated visual feedback to diagnose mishandled voxels.

5. Conclusions

A Boeing 747 airplane is comprised of over six million parts, assembled by a custom manufacturing system, and relies on an intricate global supply chain involving 1500+ companies. Would it be possible to build recyclable systems of similar complexity on our desktops? What would the world look like if ubiquitous manufacturing systems could fabricate fully-functioning robots on demand? A nascent manufacturing technique we call Layered Assembly could be the answer to each of these questions. In this work, we demonstrated the practical application of the Layered Assembly concept by employing electroadhesive grippers, as they are inherently solid-state lower-power grippers that parallelize well for $n \times n$ arrays.

Electroadhesion required for gripping even a single voxel is a highly complex phenomenon influenced by dozens of variables. The findings yielded by the present investigation nonetheless demonstrate that electroadhesion is a viable method of astrictive prehension for the selectively parallel, multi-material gripping necessary for Layered Assembly. We further demonstrated successful selective parallel gripping of 3 × 3 mm conducting and non-conducting voxels. These results will inform design decisions of electrode geometry and larger parallel electroadhesive gripping architectures going forward. Ultimately, Layered Assembly will bring the same exponential speed increases to the manufacturing sector that Moore’s Law has brought to computing power.

Author disclosure statement

No competing financial interests exist.

Acknowledgements

The authors acknowledge Jonathan Blutinger and Felice Frankel for assistance with photographs of printed samples.

Appendix A. Supplementary data

Supplementary material related to this article can be found, in the online version, at doi:https://doi.org/10.1016/j.addma.2019.03.032.

References

[1] N. Oxman, E. Tsai, M. Firstenberg, Digital anisotropy: a variable elasticity rapid prototyping platform, Virtual Phys. Prototyp. (2012), https://doi.org/10.1080/17452759.2012.731369.
[2] F. Stute, J. Mici, L. Chamberlain, H. Lipson, Digital wood: 3D internal color texture mapping, 3D print, Addit. Manuf. (2018), https://doi.org/10.1089/3dp.2018.0078.
[3] K.A. Mumtaz, N. Hopkinson, Laser melting functionally graded composition of Waspaloy® and Zirconia powders, J. Mater. Sci. 42 (2007) 7647–7656, https://doi.org/10.1007/s10853-007-1661-3.
[4] W. Li, S. Karnati, C. Kriewall, F. Liou, J. Newkirk, K.M. Brown Taminger, W.J. Seufzer, Fabrication and characterization of a functionally graded material from Ti-6Al-4V to SS316 by laser metal deposition, Addit. Manuf. 14 (2017) 95–104, https://doi.org/10.1016/J.ADDMA.2016.12.006.
[5] B.P. Conner, G.P. Manogharan, A.N. Martof, L.M. Rodomsky, C.M. Rodomsky, D.C. Jordan, J.W. Limperos, Making sense of 3-D printing: creating a map of additive manufacturing products and services, Addit. Manuf. 1–4 (2014) 64–76, https://doi.org/10.1016/J.ADDMA.2014.08.005.
[6] ASTM, F2792-12a. Standard Terminology for Additive Manufacturing Technologies, (2012), https://doi.org/10.1520/F2792-12A.
[7] E. Malone, K. Rasa, D. Cohen, T. Isaacson, H. Lashley, H. Lipson, Freeform fabrication of zinc-air batteries and electromechanical assemblies, Rapid Prototyp. J. 10 (2004) 58–69, https://doi.org/10.1108/13552540410512543.
[8] J.T. Muth, D.M. Vogt, R.L. Truby, Y. Mengüç, D.B. Kolesky, R.J. Wood, J.A. Lewis, Embedded 3D printing of strain sensors within highly stretchable elastomers, Adv. Mater. 26 (2014) 6307–6312, https://doi.org/10.1002/adma.201400334.
[9] J. Hiller, H. Lipson, Design and analysis of digital materials for physical 3D voxel printing, Rapid Prototyp. J. 15 (2009) 137–149, https://doi.org/10.1108/13552540910943441.
[10] R. MacCurdy, A. McNicoll, H. Lipson, Bitblox: printable digital materials for electromechanical machines, Int. J. Rob. Res. 33 (2014) 1342–1360, https://doi.org/10.1177/0278364914532149.
[11] G.A. Popescu, T. Mahale, A. Gershenfeld Neil, Digital materials for digital printing, Int. Conf. Digit. Fabr. Technol., Denver CO, (2006), p. 3 (Accessed April 19, 2018), http://cba.mit.edu/docs/papers/06.09.digital_materials.pdf.
[12] D. Dikovsky, Multi-material 3D printing, RadTech - Assoc. UV EB Curing Technol. (2015), p. 14 (Accessed April 24, 2018), https://www.slideshare.net/radtechuveb/multimaterial-3d-printing.
[13] W. Langford, A. Ghassaei, N. Gershenfeld, Automated assembly of electronic digital materials, Vol. 2 Mater. Biomanufacturing; Prop. Appl. Syst. Sustain. Manuf. (2016), https://doi.org/10.1115/MSEC2016-8627 p. V002T01A013.
[14] C.E. Owens, A.J. Hart, High-precision modular microfluidics by micromilling of interlocking injection-molded blocks, Lab Chip 18 (2018) 890–901, https://doi.org/10.1039/C7LC00951H.
[15] N.A. Gershenfeld, When Things Start to Think, Henry Holt, 1999.
[16] Application System Genkotsu-robot 2 High Speed Picking and Assembly Robot, (2015) (Accessed April 18, 2018), http://www.fanucamerica.com/cmsmedia/datasheets/M-2iASeries_167.pdf.

[17] G.J. Monkman, Wiley InterScience (Online Service), Robot Grippers, Wiley-VCH, 2007 (Accessed May 27, 2018), https://www.wiley.com/en-us/Robot+Grippers-p-9783527406197.
[18] G. Monkman, An analysis of astrictive prehesion, Int. J. Rob. Res. 16 (1997).
[19] H. Lipson, J. Hiller, C. Perich, S. Bernard, R. MacCurdy, F. Apoorva, Rapid Assemblers for Voxel-Based VLSI Robotics, (2014) (Accessed May 28, 2018), http://www.dtic.mil/get-tr-doc/pdf?AD=ADA624831.
[20] C. Perich, R. MacCurdy, A. Macner, J. Mici, P.H. Steen, H. Lipson, Parallel manipulation of millimeter-scale components using electro-osmotically controlled droplet arrays, IEEE Trans. Autom. Sci. Eng. (2019).
[21] B.C. Leung, N.R. Goeser, L.A. Miller, S. Gonzalez, Validation of electroadhesion as a docking method for spacecraft and satellite servicing, IEEE Aerosp. Conf. Proc. 2015–June (2015), https://doi.org/10.1109/AERO.2015.7119283.
[22] J. Guo, T. Bamber, T. Hovell, M. Chamberlain, L. Justham, M. Jackson, Geometric optimisation of electroadhesive actuators based on 3D electrostatic simulation and its experimental verification, IFAC-PapersOnLine 49 (2016) 309–315, https://doi.org/10.1016/j.ifacol.2016.10.574.
[23] J. Hiller, H. Lipson, Methods of parallel voxel manipulation for 3D digital printing, 18th Annu. Solid Free. Fabr. Symp. (2007), pp. 200–211 (Accessed April 18, 2018), https://sffsymposium.engr.utexas.edu/Manuscripts/2007/2007-17-Hiller.pdf.
[24] R. Batra, H. Lipson, Transforming lunar regolith into a digital printable material, Sp. Resour. Roundtable Planet. Terr. Min. Sci. Symp. Seventh Jt. Meet. (2016) p. 1,2.
[25] J. Guo, M. Tailor, T. Bamber, M. Chamberlain, L. Justham, M. Jackson, Investigation of relationship between interfacial electroadhesive force and surface texture, J. Phys. D Appl. Phys. 49 (2016) 2, https://doi.org/10.1088/0022-3727/49/3/035303.
[26] D. Ruffatto, J. Shah, M. Spenko, Increasing the adhesion force of electrostatic adhesives using optimized electrode geometry and a novel manufacturing process, J. Electrostat. 72 (2014) 147–155, https://doi.org/10.1016/j.elstat.2014.01.001.
[27] G. Monkman, Electroadhesive microgrippers, Ind. Robot Int. J. 30 (2003) 326–330, https://doi.org/10.1108/01439910310479595.
[28] C. Cao, X. Sun, Y. Fang, Q.H. Qin, A. Yu, X.Q. Feng, Theoretical model and design of electroadhesive pad with interdigitated electrodes, Mater. Des. 89 (2016) 485–491, https://doi.org/10.1016/j.matdes.2015.09.162.
[29] Rui Chen, Rong Liu, Hua Shen, Modeling and analysis of electric field and electrostatic adhesion force generated by interdigital electrodes for wall climbing robots, 2013 IEEE/RSJ Int. Conf. Intell. Robot. Syst., IEEE (2013) 2327–2332, https://doi.org/10.1109/IROS.2013.6696682.
[30] Inventables Inc, (n.d.). https://www.inventables.com/technologies/x-carve (Accessed April 18, 2018).
[31] Cellular Machines - Creative Machines Lab - Columbia University, (2018) (n.d.). https://www.creativemachineslab.com/cellular-machines.html (Accessed July 17, 2018).